

Effective-Lagrangian study of $\psi'(J/\psi) \rightarrow VP$ and the insights into the $\rho\pi$ puzzle

Lin-Wan Yan¹, Yun-Hua Chen², Chun-Gui Duan¹, and Zhi-Hui Guo^{1,*}

¹Department of Physics and Hebei Key Laboratory of Photophysics Research and Application, Hebei Normal University, Shijiazhuang 050024, China

²School of Mathematics and Physics, University of Science and Technology Beijing, Beijing 100083, China

 (Received 13 January 2023; accepted 30 January 2023; published 23 February 2023)

Within the effective Lagrangian approach, we carry out a unified study of the $J/\psi(\psi') \rightarrow VP$, $J/\psi \rightarrow P\gamma$ and relevant radiative decays of light-flavor hadrons. A large amount of experimental data, including the various decay widths and electromagnetic form factors, is fitted to constrain the numerous hadron couplings. Relative strengths between the strong and electromagnetic interactions are revealed in the $J/\psi \rightarrow VP$ and $\psi' \rightarrow VP$ processes. The effect from the strong interaction is found to dominate in the $J/\psi \rightarrow \rho\pi$ decay, while the electromagnetic interaction turns out to be the dominant effect in $\psi' \rightarrow \rho\pi$ decay, which provides an explanation to the $\rho\pi$ puzzle. For the $J/\psi \rightarrow K^*\bar{K} + \bar{K}^*K$ and $\psi' \rightarrow K^*\bar{K} + \bar{K}^*K$, the former process is dominated by the strong interactions, and the effects from the electromagnetic parts are found to be comparable with those of strong interactions in the latter process. Different $SU(3)$ breaking effects from the electromagnetic parts appear in the charged and neutral channels for the $\psi' \rightarrow K^*\bar{K} + \bar{K}^*K$ processes explain the rather different ratios between $B(\psi' \rightarrow K^{*+}K^- + K^{*-}K^+)/B(J/\psi \rightarrow K^{*+}K^- + K^{*-}K^+)$ and $B(\psi' \rightarrow K^{*0}\bar{K}^0 + \bar{K}^{*0}K^0)/B(J/\psi \rightarrow K^{*0}\bar{K}^0 + \bar{K}^{*0}K^0)$.

DOI: 10.1103/PhysRevD.107.034022

I. INTRODUCTION

The strong suppression of the branching ratios of the $\psi' \rightarrow \rho\pi$ and $\psi' \rightarrow K^*\bar{K} + \text{c.c.}$ processes, relative to those of the corresponding decay channels of the J/ψ , has been a long-standing puzzle in charmonium physics. The annihilation of the $c\bar{c}$ into three gluons is usually assumed to be the dominant mechanism that rules the decays of the J/ψ and ψ' to the light-flavor hadrons [1–3]. The annihilation amplitudes of the latter processes and also the decays to the lepton pairs are proportional to the wave functions of the S -wave charmonium states J/ψ and ψ' at the origin. As a result, the branching ratios with the light-flavor-hadron (h) decays of the ψ' and J/ψ can be predicted by their leptonic decay widths [4], i.e.,

$$Q_h \equiv \frac{B(\psi' \rightarrow h)}{B(J/\psi \rightarrow h)} = \frac{B(\psi' \rightarrow e^+e^-)}{B(J/\psi \rightarrow e^+e^-)} = (13.3 \pm 0.4)\%. \quad (1)$$

*Corresponding author.
zhguo@hebtu.edu.cn

Published by the American Physical Society under the terms of the Creative Commons Attribution 4.0 International license. Further distribution of this work must maintain attribution to the author(s) and the published article's title, journal citation, and DOI. Funded by SCOAP³.

However, according to the recent PDG averages [4], the ratio of $Q_{\rho\pi}$,

$$\frac{B(\psi' \rightarrow \rho\pi)}{B(J/\psi \rightarrow \rho\pi)} = (0.2 \pm 0.1)\%, \quad (2)$$

and the various ratios of $Q_{K^*\bar{K}}$,

$$\begin{aligned} \frac{B(\psi' \rightarrow K^{*+}K^- + \text{c.c.})}{B(J/\psi \rightarrow K^{*+}K^- + \text{c.c.})} &= (0.5_{-0.1}^{+0.2})\%, \\ \frac{B(\psi' \rightarrow K^{*0}\bar{K}^0 + \text{c.c.})}{B(J/\psi \rightarrow K^{*0}\bar{K}^0 + \text{c.c.})} &= (2.6_{-0.7}^{+0.8})\%, \\ \frac{B(\psi' \rightarrow K^*\bar{K} + \text{c.c.})}{B(J/\psi \rightarrow K^*\bar{K} + \text{c.c.})} &= (1.4_{-0.4}^{+0.5})\%, \end{aligned} \quad (3)$$

are drastically different from the prediction in Eq. (1). These contradictions are generally referred as the $\rho\pi$ puzzle, which was first established in Ref. [5] four decades ago. Tremendous efforts have been made to address this problem, including the proposal of a vector glueball near the J/ψ mass [6], higher Fock components in the charmonium states [7], the intrinsic charm portions in the light-flavor vector ρ [8], the nodes in the wave functions [9], the meson mixing mechanisms [10], the final-state interactions [11–14]. Another important issue in those decays is the sizable $SU(3)$ breaking effects in the charged and neutral

$K^*\bar{K}$ decays of the J/ψ and ψ' . I.e., the strict $SU(3)$ flavor symmetry would give the prediction $\mathcal{Q}_{K^*+K^-+c.c.} = \mathcal{Q}_{K^*\bar{K}^0+c.c.}$, which is however severely violated according to the experimental measurements in Eq. (3).

In this work, we aim at a unified description of the processes $J/\psi(\psi') \rightarrow VP$ and $\gamma^{(*)}P$, with V and P the light-flavor vector and pseudoscalar mesons in order. In such kinds of decay processes, one needs to simultaneously take into account of the single-Okubo-Zweig-Iizuka (OZI) or even the doubly suppressed OZI strong interaction effects, the electromagnetic contributions and the $SU(3)$ flavor symmetry breaking terms. The effective Lagrangian approach can provide an excellent framework to properly include all the aforementioned effects. Regarding the well-celebrated OZI rule, a quantitative way to understand such suppression mechanism is the large N_C QCD [15]. In the effective field theory (EFT) approach, the N_C counting order can be directly related to the number of traces in the flavor space [16,17]. Typically one additional flavor trace will introduce one more $1/N_C$ suppression order to the EFT operator. The single OZI/double OZI effects can be systematically incorporated via the EFT operators with the proper numbers of flavor traces. Furthermore, the chiral EFT is constructed according to the spontaneous and explicit chiral symmetry breaking patterns of QCD. The $SU(3)$ flavor symmetry breaking effects can be then introduced through the basic building tensors of the EFT involving the small but nonvanishing light-flavor quark masses. Although the chiral power counting scheme based on the momentum expansion is not valid in the massive J/ψ or ψ' decays, the basic building blocks and methodology of the EFT Lagrangians are useful to conveniently take into account all the relevant ingredients describing the $J/\psi(\psi') \rightarrow VP$ and $J/\psi \rightarrow \gamma^{(*)}P$ processes, including the OZI strong interaction parts, the electromagnetic contributions and the $SU(3)$ flavor symmetry breaking effects. This formalism has been successfully applied to the light-flavor decay processes of $V \rightarrow P\gamma^{(*)}$, $e^+e^- \rightarrow K^*\bar{K} + c.c.$ and $J/\psi \rightarrow VP, P\gamma^{(*)}$ in a series of works in Refs. [18–20]. In this work we push forward the study along the line of this research to address the mysterious $\rho\pi$ puzzle by including similar decay processes of ψ' . In addition, we also perform the global analyses of the large amount of updated branching ratios of various decay processes from the PDG [4] and the newly measured different decay widths from the BESIII collaboration [21].

This paper is organized as follows. In Sec. II, we introduce the relevant effective Lagrangians and elaborate the calculations of the decay amplitudes. The global fit to the various experimental data and the phenomenological consequences are analyzed in detail in Sec. III. We give a short summary and conclusions in Sec. IV.

II. EFFECTIVE LAGRANGIAN AND CALCULATIONS OF TRANSITION AMPLITUDES

The primary aim of this work is to study the various decay processes of the J/ψ and ψ' into a light-flavor vector and a light pseudoscalar meson, and the light-flavor meson radiative decays and relevant form factors. Therefore we need to include not only the transition operators between the charmonia and the light-flavor mesons, but also the EFT operators describing the interactions among the light-meson themselves. To tightly constrain the free couplings, we simultaneously take into account the experimental data from both the decay processes with only light-flavor mesons and also the processes involving the J/ψ and ψ' .

Resonance chiral theory ($R\chi T$) [22] provides a reliable framework to study the interactions of the light-flavor resonances and the light pseudoscalar mesons (π, K, η), the latter of which are treated as the pseudo-Nambu-Goldstone bosons (pNGBs) resulting from the spontaneous symmetry breaking of QCD. As an extension of the chiral perturbation theory (χPT), $R\chi T$ explicitly introduces the heavier degrees of freedom of QCD, i.e., the light-flavor resonances, such as the vectors ρ, K^*, ω, ϕ , the axial vectors, scalars, etc., into the chiral Lagrangians, together with the pNGBs and external source fields, like the photons. The $R\chi T$ operators are constructed in a chiral covariant way, therefore the physical amplitudes calculated in the $R\chi T$ automatically fulfill the requirements of chiral symmetry of QCD in the low energy region. On the other hand, the large N_C expansion of QCD [15] has been widely used as another useful guide to arrange the operators and amplitudes of the $R\chi T$ [23]. In addition, from the large N_C point of view, the QCD $U_A(1)$ anomaly effect, which is considered to be the most responsible factor for the large mass of the physical state η' , is however $1/N_C$ suppressed. As a result, the η' state would become the ninth pNGB both in large N_C and chiral limits. Based on this argument, the nonet of the pNGBs (π, K, η, η') can be systematically included in the effective Lagrangian [24]. We closely follow this guideline to include the singlet η_0 state in the $R\chi T$ and adopt the general two-mixing-angle formalism to study the physical processes with the η and η' mesons. Next we briefly introduce the relevant $R\chi T$ Lagrangians.

In the present work, only the light-flavor vector resonances will be relevant to our study and the minimal interaction operators with the vectors in even-intrinsic-parity sector of the $R\chi T$ is given by [22]

$$\mathcal{L}_V^{(2)} = \frac{F_V}{2\sqrt{2}} \langle V_{\mu\nu} f_+^{\mu\nu} \rangle + i \frac{G_V}{\sqrt{2}} \langle V_{\mu\nu} u^\mu u^\nu \rangle, \quad (4)$$

where the nonet of the vector resonances is incorporated via the 3×3 matrix

$$V_{\mu\nu} = \begin{pmatrix} \frac{1}{\sqrt{2}}\rho^0 + \frac{1}{\sqrt{6}}\omega_8 + \frac{1}{\sqrt{3}}\omega_0 & \rho^+ & K^{*+} \\ \rho^- & -\frac{1}{\sqrt{2}}\rho^0 + \frac{1}{\sqrt{6}}\omega_8 + \frac{1}{\sqrt{3}}\omega_0 & K^{*0} \\ K^{*-} & \bar{K}^{*0} & -\frac{2}{\sqrt{6}}\omega_8 + \frac{1}{\sqrt{3}}\omega_0 \end{pmatrix}_{\mu\nu}, \quad (5)$$

the basic chiral tensors with the pNGBs and the external source fields are defined as

$$U = u^2 = e^{i\frac{\sqrt{2}\Phi}{F}}, \quad u_\mu = i[u^\dagger(\partial_\mu - ir_\mu)u - u(\partial_\mu - u\ell_\mu)u^\dagger], \quad f_{\pm}^{\mu\nu} = uF_L^{\mu\nu}u^\dagger \pm u^\dagger F_R^{\mu\nu}u, \\ F_{L(R)}^{\mu\nu} = \partial^\mu l(r)^\nu - \partial^\nu l(r)^\mu, \quad \chi_{\pm} = u^\dagger \chi u^\dagger \pm u \chi^\dagger u, \quad \chi = 2B_0(s + ip) \quad (6)$$

and the flavor contents of the nonet pNGB matrix read

$$\Phi = \begin{pmatrix} \frac{1}{\sqrt{2}}\pi^0 + \frac{1}{\sqrt{6}}\eta_8 + \frac{1}{\sqrt{3}}\eta_0 & \pi^+ & K^+ \\ \pi^- & -\frac{1}{\sqrt{2}}\pi^0 + \frac{1}{\sqrt{6}}\eta_8 + \frac{1}{\sqrt{3}}\eta_0 & K^0 \\ K^- & \bar{K}^0 & -\frac{2}{\sqrt{6}}\eta_8 + \frac{1}{\sqrt{3}}\eta_0 \end{pmatrix}. \quad (7)$$

The quark-mass terms are introduced by taking the scalar external source filed s in Eq. (6) as $s = \text{diag}\{m_u, m_d, m_s\}$. In this work, we will take $m_u = m_d = \hat{m}$ throughout, i.e., neglecting the isospin breaking effects from the strong interaction parts. The physical vectors ω and ϕ can be well described by assuming the ideal mixing of the octet ω_8 and the singlet ω_0 [4]

$$\omega_0 = \sqrt{\frac{2}{3}}\omega - \sqrt{\frac{1}{3}}\phi, \\ \omega_8 = \sqrt{\frac{2}{3}}\phi + \sqrt{\frac{1}{3}}\omega. \quad (8)$$

In contrast, the mixing pattern of the η_8 and η_0 is more involved. The modern chiral prescription introduces the sophisticated two-mixing-angle scheme [25,26] to address the $\eta - \eta'$ mixing system

$$\begin{pmatrix} \eta \\ \eta' \end{pmatrix} = \frac{1}{F} \begin{pmatrix} F_8 \cos \theta_8 & -F_0 \sin \theta_0 \\ F_8 \sin \theta_8 & F_0 \cos \theta_0 \end{pmatrix} \begin{pmatrix} \eta_8 \\ \eta_0 \end{pmatrix}, \quad (9)$$

where F_0 and F_8 are the weak decay constants of the singlet and octet axial-vector currents, respectively. The conventional mixing formula with a single mixing angle can be naturally recovered by taking $F_8 = F_0 = F$ and $\theta_0 = \theta_8$ in Eq. (9). Equivalently one can also use the quark-flavor basis to describe the two-mixing-angle formalism

$$\begin{pmatrix} \eta \\ \eta' \end{pmatrix} = \frac{1}{F} \begin{pmatrix} F_q \cos \theta_q & -F_s \sin \theta_s \\ F_q \sin \theta_q & F_s \cos \theta_s \end{pmatrix} \begin{pmatrix} \eta_q \\ \eta_s \end{pmatrix}, \quad (10)$$

where the quark-flavor contents of the states $\eta_q = (\eta_8 + \sqrt{2}\eta_0)/\sqrt{3}$ and $\eta_s = (-\sqrt{2}\eta_8 + \eta_0)/\sqrt{3}$ are $(\bar{u}u + \bar{d}d)/\sqrt{2}$ and $\bar{s}s$, respectively.

The vector resonances in Eq. (4) are expressed in terms of the antisymmetric tensors, instead of the commonly used Proca fields. It is demonstrated in Refs. [22,27] that it is convenient to use the antisymmetric tensors to describe the vector resonances in $R\chi T$, since the high energy behaviors of the resulting amplitudes and form factors automatically match the QCD constraints without requiring the inclusion of extra local chiral counterterms in the antisymmetric tensor formalism. The $R\chi T$ Lagrangians in the odd-intrinsic-parity sector comprise two different classes, namely the VVP and VJP types, with J the external sources. Those $R\chi T$ operators written in terms of the antisymmetric tensor fields that are relevant to the $O(p^4)$ chiral low energy constants, are worked out in Ref. [28], and the relevant $R\chi T$ Lagrangians and discussions on the VVP Green functions by explicitly including the dynamical singlet η_0 state are given in Ref. [18]. A more complete basis of the odd-intrinsic-parity $R\chi T$ operators that contribute to the $O(p^6)$ chiral low energy constants, is given in Ref. [29]. A proliferation of the unknown resonance couplings arise in the more complete $R\chi T$ Lagrangians, as expected. This can hinder one from giving the definite conclusions on the phenomenological discussions [30]. From the practical point of view, we will work with the $R\chi T$ operator basis from Refs. [18,28] and we believe that the higher order effects from the extra operators in Ref. [29] can be accounted for by the uncertainties of the resonance couplings in the former two references. For the sake of completeness, we give the explicit expressions of the relevant $R\chi T$ Lagrangians [18,28]

$$\begin{aligned} \mathcal{L}_{VVP} = & d_1 \varepsilon_{\mu\nu\rho\sigma} \langle \{V^{\mu\nu}, V^{\rho\alpha}\} \nabla_\alpha u^\sigma \rangle + id_2 \varepsilon_{\mu\nu\rho\sigma} \langle \{V^{\mu\nu}, V^{\rho\sigma}\} \chi_- \rangle + d_3 \varepsilon_{\mu\nu\rho\sigma} \langle \{ \nabla_\alpha V^{\mu\nu}, V^{\rho\alpha} \} u^\sigma \rangle \\ & + d_4 \varepsilon_{\mu\nu\rho\sigma} \langle \{ \nabla^\sigma V^{\mu\nu}, V^{\rho\alpha} \} u_\alpha \rangle - id_5 M_V^2 \sqrt{\frac{2}{3}} \varepsilon_{\mu\nu\rho\sigma} \langle V^{\mu\nu} V^{\rho\sigma} \rangle \ln(\det u), \end{aligned} \quad (11)$$

and

$$\begin{aligned} \mathcal{L}_{VJP} = & \frac{c_1}{M_V} \varepsilon_{\mu\nu\rho\sigma} \langle \{V^{\mu\nu}, f_+^{\rho\alpha}\} \nabla_\alpha u^\sigma \rangle + \frac{c_2}{M_V} \varepsilon_{\mu\nu\rho\sigma} \langle \{V^{\mu\alpha}, f_+^{\rho\sigma}\} \nabla_\alpha u^\nu \rangle + \frac{ic_3}{M_V} \varepsilon_{\mu\nu\rho\sigma} \langle \{V^{\mu\nu}, f_+^{\rho\sigma}\} \chi_- \rangle \\ & + \frac{ic_4}{M_V} \varepsilon_{\mu\nu\rho\sigma} \langle V^{\mu\nu} [f_-^{\rho\sigma}, \chi_+] \rangle + \frac{c_5}{M_V} \varepsilon_{\mu\nu\rho\sigma} \langle \{ \nabla_\alpha V^{\mu\nu}, f_+^{\rho\alpha} \} u^\sigma \rangle + \frac{c_6}{M_V} \varepsilon_{\mu\nu\rho\sigma} \langle \{ \nabla_\alpha V^{\mu\alpha}, f_+^{\rho\sigma} \} u^\nu \rangle \\ & + \frac{c_7}{M_V} \varepsilon_{\mu\nu\rho\sigma} \langle \{ \nabla^\sigma V^{\mu\nu}, f_+^{\rho\alpha} \} u_\alpha \rangle - ic_8 M_V \sqrt{\frac{2}{3}} \varepsilon_{\mu\nu\rho\sigma} \langle V^{\mu\nu} \tilde{f}_+^{\rho\sigma} \rangle \ln(\det u), \end{aligned} \quad (12)$$

where the covariant derivative acting on the chiral field X is given by

$$\begin{aligned} \nabla_\mu X &= \partial_\mu X + [\Gamma_\mu, X], \\ \Gamma_\mu &= \frac{1}{2} [u^+ (\partial_\mu - ir_\mu) u + u (\partial_\mu - il_\mu) u^+]. \end{aligned} \quad (13)$$

As previously mentioned in the Introduction, both the strong and electromagnetic interactions can be important in the $J/\psi(\psi') \rightarrow VP$ processes. The effects from the strong interactions are taken into account by the direct $J/\psi(\psi')VP$ transition operators [18]

$$\begin{aligned} \mathcal{L}_{\psi(\psi')VP} = & M_{\psi(\psi')VP} h_1^{(\prime)} \varepsilon_{\mu\nu\rho\sigma} \psi^{(\prime)\mu} \langle u^\nu V^{\rho\sigma} \rangle \\ & + \frac{1}{M_{\psi(\psi')}} h_2^{(\prime)} \varepsilon_{\mu\nu\rho\sigma} \psi^{(\prime)\mu} \langle \{u^\nu, V^{\rho\sigma}\} \chi_+ \rangle \\ & + M_{\psi(\psi')} h_3^{(\prime)} \varepsilon_{\mu\nu\rho\sigma} \psi^{(\prime)\mu} \langle u^\nu \rangle \langle V^{\rho\sigma} \rangle, \end{aligned} \quad (14)$$

where the couplings $h_{i=1,2,3}^{(\prime)}$ corresponding to the J/ψ and ψ' will be separately fitted to the experimental data of the two charmonium states. Two types of EFT operators are introduced to account for the electromagnetic effects, which include the direct $\psi P\gamma$ transition operators

$$\mathcal{L}_{\psi P\gamma} = g_1 \varepsilon_{\mu\nu\rho\sigma} \psi^\mu \langle u^\nu f_+^{\rho\sigma} \rangle + \frac{1}{M_\psi^2} g_2 \varepsilon_{\mu\nu\rho\sigma} \psi^\mu \langle \{u^\nu, f_+^{\rho\sigma}\} \chi_+ \rangle, \quad (15)$$

and the conversion vertex of the charmonium and the photon

$$\mathcal{L}_{\psi\gamma} = \frac{-1}{2\sqrt{2}M_\psi} f_\psi \langle \hat{\psi}_{\mu\nu} f_+^{\mu\nu} \rangle, \quad (16)$$

being $\hat{\psi}_{\mu\nu} = \partial_\mu \psi_\nu - \partial_\nu \psi_\mu$. The values of the couplings g_1 , g_2 , and f_ψ are different for the J/ψ and ψ' and they will be determined by the relevant experimental data. Different powers of the $M_{\psi(\psi')}$ are introduced in Eqs. (14)–(16), so

that the couplings appearing in those Lagrangians are dimensionless.

It is found [20,31] that the $J/\psi \rightarrow \eta^{(\prime)}\gamma^{(*)}$ amplitudes are dominated by the η_c mediating diagrams, i.e., via the $J/\psi \rightarrow \eta_c\gamma^{(*)} \rightarrow \eta^{(\prime)}\gamma^{(*)}$ intermediate processes. The decay amplitude of the $\psi \rightarrow \eta^{(\prime)}\gamma^{(*)}$ can be written as

$$\mathcal{M}_{\psi \rightarrow \eta^{(\prime)}\gamma^{(*)}}^{\text{mixing}} = e \varepsilon_{\mu\nu\rho\sigma} \epsilon_\psi^\mu \epsilon_{\gamma^{(*)}}^\nu q^\rho k^\sigma \lambda_{\eta_c\eta^{(\prime)}} g_{\psi\eta_c\gamma^{(*)}}(s) e^{i\delta_P}, \quad (17)$$

being $P = \eta, \eta'$, where the electromagnetic transition form factor between the ψ and η_c takes form [32–34]

$$g_{\psi\eta_c\gamma^{(*)}}(s) = g_{\psi\eta_c\gamma^{(*)}}(0) e^{\frac{s}{16\beta^2}}. \quad (18)$$

For the mixing parameters $\lambda_{\eta_c\eta^{(\prime)}}$ between the η_c and $\eta^{(\prime)}$ states, we take the determinations $\lambda_{\eta_c\eta} = -4.6 \times 10^{-3}$ and $\lambda_{\eta_c\eta'} = -1.2 \times 10^{-2}$ from Ref. [31]. The phenomenological phase factors $\delta_{\eta^{(\prime)}}$ in front of the η_c mediating diagrams need to be separately fitted to the data of the J/ψ .

The various Feynman diagrams relevant to our study are illustrated in Figs. 1–3. To be more specific, the diagrams in Fig. 1 contribute to the light-flavor processes $V \rightarrow P\gamma^{(*)}$ and $P \rightarrow V\gamma^{(*)}$. The amplitudes of the $J/\psi(\psi') \rightarrow VP$ and $J/\psi \rightarrow P\gamma^{(*)}$ receive contributions from the diagrams in Figs. 2 and 3, respectively. The formulas relevant to the $V \rightarrow P\gamma^{(*)}$ and $P \rightarrow V\gamma^{(*)}$ processes are worked out in Ref. [18], and the expressions of the $J/\psi \rightarrow VP, P\gamma^{(*)}$

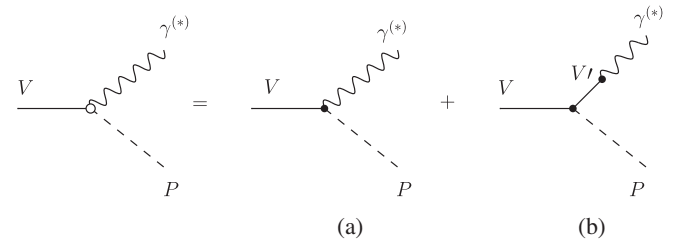


FIG. 1. Diagrams relevant to the $V \rightarrow P\gamma^{(*)}$ processes: (a) direct type and (b) indirect type.

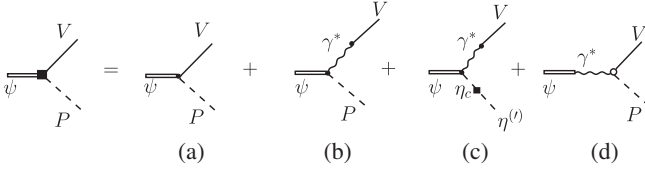


FIG. 2. Feynman diagrams for the processes $J/\psi \rightarrow VP$: (a) the strong-interaction contributions from the $h_{i=1,2,3}$ terms; (b) the electromagnetic contributions from the $g_{i=1,2}$ terms; (c) the η_c mediated part; (d) the contributions from the $\gamma^* \rightarrow VP$ vertexes. See the text for details.

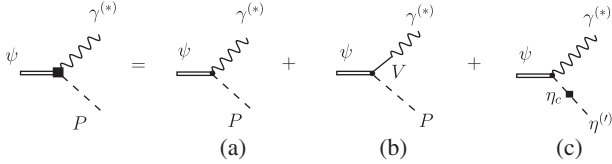


FIG. 3. Feynman diagrams for the processes $J/\psi \rightarrow P\gamma^{(*)}$: (a) the direct type; (b) the light-vector mediated part; (c) the η_c mediated part.

amplitudes are calculated in Ref. [20]. The corresponding decay amplitudes of the ψ' state share similar expressions as those involving J/ψ , with obvious replacements of the resonance couplings. Nevertheless, for the sake of completeness and to set up the notations, we further elaborate the amplitudes of the processes of $\psi' \rightarrow VP$.

For the $\psi' \rightarrow VP$ decay, the first diagram (a) in Fig. 2 denotes the contributions from the strong interactions, i.e., from the Lagrangians in Eq. (14). Other diagrams in Fig. 2 correspond to the electromagnetic effects. The $\psi' \rightarrow VP$ amplitude can be written as

$$\mathcal{M}_{\psi' \rightarrow VP} = \varepsilon_{\mu\nu\rho\sigma} \epsilon_{\psi'}^{\mu} \epsilon_V^{\nu} q^{\rho} k^{\sigma} G_{\psi' \rightarrow VP}, \quad (19)$$

where the polarization vectors of the ψ' and V are given by $\epsilon_{\psi'}^{\mu}$ and ϵ_V^{ν} , q and k stand for the four-momentum of the ψ' and V , respectively. The effective couplings $G_{\psi' \rightarrow VP}$ include various contributions from the individual diagram of Fig. 2. The explicit expressions of $G_{\psi' \rightarrow VP}$ for the various processes are given in the Appendix. The decay widths of $\psi' \rightarrow VP$ read

$$\Gamma(\psi' \rightarrow VP) = \frac{1}{96\pi M_{\psi'}^3} \lambda(M_{\psi'}, M_V, m_P)^{\frac{3}{2}} |G_{\psi' \rightarrow VP}|^2, \quad (20)$$

with the Källén function $\lambda(x, y, z) = x^2 + y^2 + z^2 - 2xy - 2xz - 2yz$.

Similarly, the corresponding amplitude of the radiative process $J/\psi(q) \rightarrow \gamma^*(k)P(q-k)$ can be given in terms of one effective coupling as well

$$\mathcal{M}_{\psi \rightarrow P\gamma^*} = e \varepsilon_{\mu\nu\rho\sigma} \epsilon_{\psi}^{\mu} \epsilon_{\gamma^*}^{\nu} q^{\rho} k^{\sigma} G_{\psi \rightarrow P\gamma^*}(s), \quad (21)$$

with $s = k^2$. The effective coupling $G_{\psi \rightarrow P\gamma^*}$ can receive contributions from all the diagrams in Fig. 3. The explicit expressions are given in Ref. [20]. The formula of the decay width of the $J/\psi \rightarrow P\gamma$ process finds it form

$$\Gamma_{\psi \rightarrow P\gamma} = \frac{1}{3} \alpha \left(\frac{M_{\psi}^2 - M_P^2}{2M_{\psi}} \right)^3 |G_{\psi \rightarrow P\gamma^*}(0)|^2. \quad (22)$$

The expression of the width for the Dalitz decay process $J/\psi \rightarrow P\gamma^* \rightarrow Pl^+l^-$ is given by

$$\Gamma_{\psi \rightarrow Pl^+l^-} = \int_{4m_l^2}^{(M_{\psi}-m_P)^2} \frac{\alpha^2 (2m_l^2 + s)}{72M_{\psi}^3 \pi s^3} \sqrt{s(s-4m_l^2)} \times [\lambda(s, M_{\psi}, m_P)]^{\frac{3}{2}} |G_{\psi \rightarrow P\gamma^*}(s)|^2 ds. \quad (23)$$

III. COMPREHENSIVE FITS AND PHENOMENOLOGICAL DISCUSSIONS

Compared to the previous studies in Refs. [18,20], we incorporate in this work the data from the various $\psi' \rightarrow VP$ decays, apart from other types of data from the $V \rightarrow P\gamma^{(*)}$, $P \rightarrow V\gamma^{(*)}$, and $J/\psi \rightarrow VP, P\gamma^{(*)}$ processes, to perform a comprehensive fit, so that the $\rho\pi$ puzzle can be addressed. In addition, we update numerous types of data according to the most recent PDG averages [4], and timely revise the determinations of the resonance couplings.

In total, we include 135 data points from several different types of processes in the comprehensive fit. To be more specific, the data from the pure light-flavor processes amount to 70, and they consist of both the decay widths, such as those of the $\omega \rightarrow \eta\gamma$, $\eta' \rightarrow \omega\gamma$, $\eta \rightarrow \gamma\gamma$, etc., and the form factors of the $\phi \rightarrow \eta\gamma^*$ and $\eta^{(\prime)} \rightarrow \gamma\gamma^*$. For the data related to the J/ψ , they include all the available widths of the $J/\psi \rightarrow VP, P\gamma$, and Pe^+e^- from the PDG [4], and also the recent BESIII measurements of the invariant-mass distributions of the lepton pairs in the transition of $J/\psi \rightarrow \eta\gamma^*$ [21]. Regarding the data of the ψ' , we will include in the joint fit all the available widths of the $\psi' \rightarrow VP$ processes from PDG [4].

An efficient way to reduce the number of unknown couplings in the R χ T is to impose the high energy constraints dictated by QCD to the various form factors and Green functions calculated from the R χ T Lagrangians in Eqs. (4), (11) and (12). Furthermore, the high energy behaviors of the resulting amplitudes after imposing such constraints will mimic the properties as predicted by QCD. Following the previous discussions in Refs. [18–20,28,35–37], we take the following high energy constraints on the various couplings

$$\begin{aligned}
4c_3 + c_1 = 0, \quad c_1 - c_2 + c_5 = 0, \quad c_5 - c_6 = \frac{N_C}{64\pi^2} \frac{M_V}{\sqrt{2}F_V}, \\
d_1 + 8d_2 - d_3 = \frac{F^2}{8F_V^2}, \quad d_3 = -\frac{N_C}{64\pi^2} \frac{M_V^2}{F_V^2}, \quad c_8 = -\frac{\sqrt{2}M_0^2}{\sqrt{3}M_V^2} c_1,
\end{aligned} \tag{24}$$

where the pion weak decay constant takes the normalization $F = 92.4$ MeV throughout, the $U_A(1)$ anomaly parameter is set to be $M_0 = 900$ MeV [38,39], the chiral-limit mass of the lowest vector resonance multiplet is fixed at $M_V = M_\rho = 775$ MeV and the vector-photon transition coupling F_V will be fitted. By taking into account the leptonic widths of the J/ψ and ψ' , we can determine the charmonium-photon transition coupling $f_{J/\psi(\psi')}$ in Eq. (16), whose explicit values are found to be

$$f_{J/\psi} = 293.8 \pm 3.5 \text{ MeV}, \quad f_{\psi'} = 208.1 \pm 5.1 \text{ MeV}. \tag{25}$$

We are then left with 23 undetermined parameters, including the four η - η' mixing parameters introduced in Eq. (9), four couplings F_V , c_3 , c_4 , and d_2 that emerge from the light-flavor resonance interactions, nine parameters exclusively entering in the J/ψ decays and six parameters that are dedicated to the ψ' processes. The couplings that describe the interactions of the light-flavor resonances will also enter in the charmonia decays. Therefore the joint fits by simultaneously including the relevant data of the light-flavor mesons, the data from the $J/\psi \rightarrow VP, P\gamma^{(*)}$ and the ψ' ones, will obviously give more stringent constraints on the couplings than the situation by including just one of these datasets. Furthermore, such comprehensive studies in a unified framework are also expected to give a further insight into $\rho\pi$ puzzle elaborated in the Introduction.

The resulting parameters from the joint fit are given in Table I. The updated parameters related to the light-flavor resonances, the J/ψ decays and the $\eta - \eta'$ mixing are well

consistent with the previous determinations [18–20] where the data of the ψ' processes are not included in these studies. For the $\psi' \rightarrow P\gamma^{(*)}$ processes, which could receive significant contributions from the $\psi' \rightarrow J/\psi P$ transition vertexes, i.e., $\psi' \rightarrow J/\psi\eta \rightarrow \gamma\eta$ [40], are not considered in this work. Therefore we will not discuss such kinds of processes here. The relative phases $\delta_{\eta^{(\prime)}}$ of Eq. (17) for the η_c mediating effects in the $\psi' \rightarrow V\eta^{(\prime)}$ decay processes, are found to be insensitive to our present studies. As a result, the phases of $\delta_{\eta^{(\prime)}}$ in the ψ' decays will be fixed to zero throughout. The previous study in Ref. [18] pointed out a strong correlation between the d_2 and d_5 parameters, and we find that this correlation still holds in our joint fit. The resulting relation turns out to be $d_5 = 3.57d_2 + 0.01$. Regarding the four parameters F_8 , F_0 , θ_8 , and θ_0 related with the $\eta - \eta'$ mixing, our current determinations of the central values and uncertainties more or less resemble those in Ref. [20]. In Ref. [18], only the data from the light-flavor sector were considered and the resulting $\eta - \eta'$ mixing parameters were found to bear large uncertainties. The simultaneous inclusion of the relevant data from the J/ψ and ψ' processes, together with the light-flavor ones, can obviously pin down the uncertainties of the $\eta - \eta'$ mixing parameters [20,41–43]. In Table I, we also give the predictions to the mixing parameters in the quark-flavor basis.

Generally speaking, the numerous types of data are well reproduced in our comprehensive fit. The comparisons of the various decay widths for the pure light-flavor processes

TABLE I. Parameters from the joint fit. The quantities marked with asterisk are predictions, instead of free parameters in the fit.

F_8	$(1.41 \pm 0.02)F_\pi$	F_0	$(1.36 \pm 0.03)F_\pi$
θ_8	$(-24.3 \pm 0.4)^\circ$	θ_0	$(-12.8 \pm 0.5)^\circ$
F_V	139.04 ± 1.72	c_3	0.0046 ± 0.0003
c_4	-0.0014 ± 0.0001	d_2	0.100 ± 0.008
h_1	$(-2.35 \pm 0.06) \times 10^{-5}$	h_2	$(-3.08 \pm 0.60) \times 10^{-5}$
h_3	$(3.39 \pm 0.22) \times 10^{-6}$	g_1	$(-2.40 \pm 0.06) \times 10^{-5}$
g_2	$(-2.23 \pm 0.48) \times 10^{-4}$	r_1	0.40 ± 0.04
h'_1	$(0.33 \pm 0.23) \times 10^{-6}$	h'_2	$(-4.01 \pm 0.32) \times 10^{-5}$
h'_3	$(0.85 \pm 0.47) \times 10^{-6}$	g'_1	$(-1.70 \pm 0.47) \times 10^{-4}$
g'_2	$(0.18 \pm 0.95) \times 10^{-3}$	δ_η	$(117.12 \pm 3.81)^\circ$
$\delta_{\eta'}$	$(50.03 \pm 16.01)^\circ$	β	$512.86 \pm 7.36 \text{ MeV}$
β'	$112.97 \pm 0.98 \text{ MeV}$	$F_q^{(*)}$	$(1.24 \pm 0.02)F_\pi$
$F_s^{(*)}$	$(1.52 \pm 0.02)F_\pi$	$\theta_q^{(*)}$	$(37.3 \pm 0.7)^\circ$
$\theta_s^{(*)}$	$(35.1 \pm 0.4)^\circ$	$\chi^2/\text{d.o.f}$	$157.25/(135 - 23) = 1.40$

TABLE II. The decay widths in units of KeV for the light-flavor hadrons.

	Experiment	Fit
$\Gamma_{\omega \rightarrow \pi\gamma}$	724.78 ± 34.64	705.65 ± 17.40
$\Gamma_{\rho^0 \rightarrow \pi^0\gamma}$	70.08 ± 12.37	73.23 ± 1.81
$\Gamma_{K^{*0} \rightarrow K^0\gamma}$	116.36 ± 11.27	108.95 ± 2.69
$\Gamma_{\omega \rightarrow \pi e^- e^+}$	6.68 ± 0.63	6.40 ± 0.16
$\Gamma_{\omega \rightarrow \pi \mu^- \mu^+}$	1.16 ± 0.18	0.63 ± 0.02
$\Gamma_{\omega \rightarrow \eta\gamma}$	3.91 ± 0.41	5.30 ± 0.11
$\Gamma_{\rho^0 \rightarrow \eta\gamma}$	44.73 ± 3.39	43.93 ± 0.96
$\Gamma_{\phi \rightarrow \eta\gamma}$	55.28 ± 1.23	55.01 ± 1.00
$\Gamma_{\phi \rightarrow \eta'\gamma}$	0.26 ± 0.01	0.26 ± 0.01
$\Gamma_{\eta' \rightarrow \omega\gamma}$	4.74 ± 0.29	5.05 ± 0.18
$\Gamma_{\eta \rightarrow \gamma\gamma}$	0.52 ± 0.02	0.50 ± 0.01
$\Gamma_{\eta' \rightarrow \gamma\gamma}$	4.34 ± 0.20	3.92 ± 0.11
$\Gamma_{\eta \rightarrow \gamma e^- e^+}$	$(9.04 \pm 0.89) \times 10^{-3}$	$(8.32 \pm 0.23) \times 10^{-3}$
$\Gamma_{\eta \rightarrow \gamma \mu^- \mu^+}$	$(0.41 \pm 0.07) \times 10^{-3}$	$(0.39 \pm 0.01) \times 10^{-3}$
$\Gamma_{\eta' \rightarrow \gamma \mu^- \mu^+}$	$(2.12 \pm 0.61) \times 10^{-2}$	$(1.47 \pm 0.04) \times 10^{-2}$
$\Gamma_{\phi \rightarrow \eta e^- e^+}$	0.459 ± 0.018	0.460 ± 0.008

from the revised fit and the updated PDG values are shown in Table II. Similar comparisons for the partial decay widths of the J/ψ and ψ' are given in Tables III and IV, respectively. The resulting curves of the form factors for the $\eta \rightarrow \gamma\gamma^*$, $\eta' \rightarrow \gamma\gamma^*$, $\phi \rightarrow \eta\gamma^*$ and $J/\psi \rightarrow \eta'\gamma^*$ are shown together with the experimental data in Fig. 4. The fitted results of the recent BESIII measurements on the e^+e^- spectra in the $J/\psi \rightarrow \eta e^+e^-$ processes are illustrated in Fig. 5. We point out a subtlety about the effects of the light-flavor vector resonances in the e^+e^- spectra. In the $J/\psi \rightarrow \eta' e^+e^-$ decays, the light-flavor vectors are removed in the

TABLE IV. Branching fractions($\times 10^{-3}$) of the decay processes for ψ' . The $\psi' \rightarrow \omega\eta$ channel is not included in the fit, instead the result corresponds to our prediction, which is around two times smaller than the upper limit 1.1×10^{-5} reported in PDG [4].

	Experiment	Fit
$\psi' \rightarrow \rho\pi$	0.032 ± 0.012	0.037 ± 0.010
$\psi' \rightarrow \rho^0\eta$	0.022 ± 0.006	0.021 ± 0.005
$\psi' \rightarrow \rho^0\eta'$	0.019 ± 0.017	0.028 ± 0.008
$\psi' \rightarrow \omega\pi^0$	0.021 ± 0.006	0.021 ± 0.004
$\psi' \rightarrow \omega\eta$...	0.005 ± 0.003
$\psi' \rightarrow \omega\eta'$	0.032 ± 0.025	0.033 ± 0.019
$\psi' \rightarrow \phi\eta$	0.031 ± 0.003	0.032 ± 0.003
$\psi' \rightarrow \phi\eta'$	0.0154 ± 0.0020	0.016 ± 0.002
$\psi' \rightarrow K^{*+}K^- + \text{c.c.}$	0.029 ± 0.004	0.029 ± 0.004
$\psi' \rightarrow K^{*0}\bar{K}^0 + \text{c.c.}$	0.109 ± 0.020	0.080 ± 0.011

BESIII analysis [44], and as a result we have also subtracted the contributions from the intermediate light vector exchanges in accord with the experimental setups. This explains the smooth line shapes of the electromagnetic $J/\psi \rightarrow \eta' e^+e^-$ transition form factors shown in Fig. 4. Regarding the $J/\psi \rightarrow \eta e^+e^-$ process, we keep the effects of the intermediate light-flavor vector resonances, in order to be consistent with the setups of the experimental analyses in Ref. [21]. It should be stressed that the prominent peaks of the narrow vectors ω and ϕ can be diluted due to the large bin widths of the experimental energy resolutions. To clearly show the influence of the bin widths, we give the histograms by using the energy bin width at 50 MeV. It is evident that the signals of narrow light vector resonances can be obviously enhanced when the energy bin width is reduced.

TABLE III. Branching fractions($\times 10^{-3}$) of the decay processes for J/ψ .

	Experiment	Fit
$J/\psi \rightarrow \rho^0\pi^0$	5.6 ± 0.7	5.5 ± 0.3
$J/\psi \rightarrow \rho\pi$	16.9 ± 1.5	16.2 ± 1.0
$J/\psi \rightarrow \rho^0\eta$	0.193 ± 0.023	0.185 ± 0.021
$J/\psi \rightarrow \rho^0\eta'$	0.081 ± 0.008	0.080 ± 0.007
$J/\psi \rightarrow \omega\pi^0$	0.45 ± 0.05	0.45 ± 0.04
$J/\psi \rightarrow \omega\eta$	1.74 ± 0.20	1.65 ± 0.09
$J/\psi \rightarrow \omega\eta'$	0.189 ± 0.018	0.189 ± 0.018
$J/\psi \rightarrow \phi\eta$	0.74 ± 0.08	0.76 ± 0.06
$J/\psi \rightarrow \phi\eta'$	0.46 ± 0.05	0.45 ± 0.05
$J/\psi \rightarrow K^{*+}K^- + \text{c.c.}$	6.0 ± 1.0	6.6 ± 0.3
$J/\psi \rightarrow K^{*0}\bar{K}^0 + \text{c.c.}$	4.2 ± 0.4	3.8 ± 0.2
$J/\psi \rightarrow \pi^0\gamma$	0.0356 ± 0.0017	0.0341 ± 0.0016
$J/\psi \rightarrow \eta\gamma$	1.085 ± 0.018	1.085 ± 0.013
$J/\psi \rightarrow \eta'\gamma$	5.25 ± 0.07	5.35 ± 0.04
$J/\psi \rightarrow \pi^0 e^+ e^-$	$(0.076 \pm 0.014) \times 10^{-2}$	$(0.129 \pm 0.004) \times 10^{-2}$
$J/\psi \rightarrow \eta e^+ e^-$	$(1.42 \pm 0.08) \times 10^{-2}$	$(1.35 \pm 0.02) \times 10^{-2}$
$J/\psi \rightarrow \eta' e^+ e^-$	$(6.59 \pm 0.18) \times 10^{-2}$	$(6.08 \pm 0.05) \times 10^{-2}$

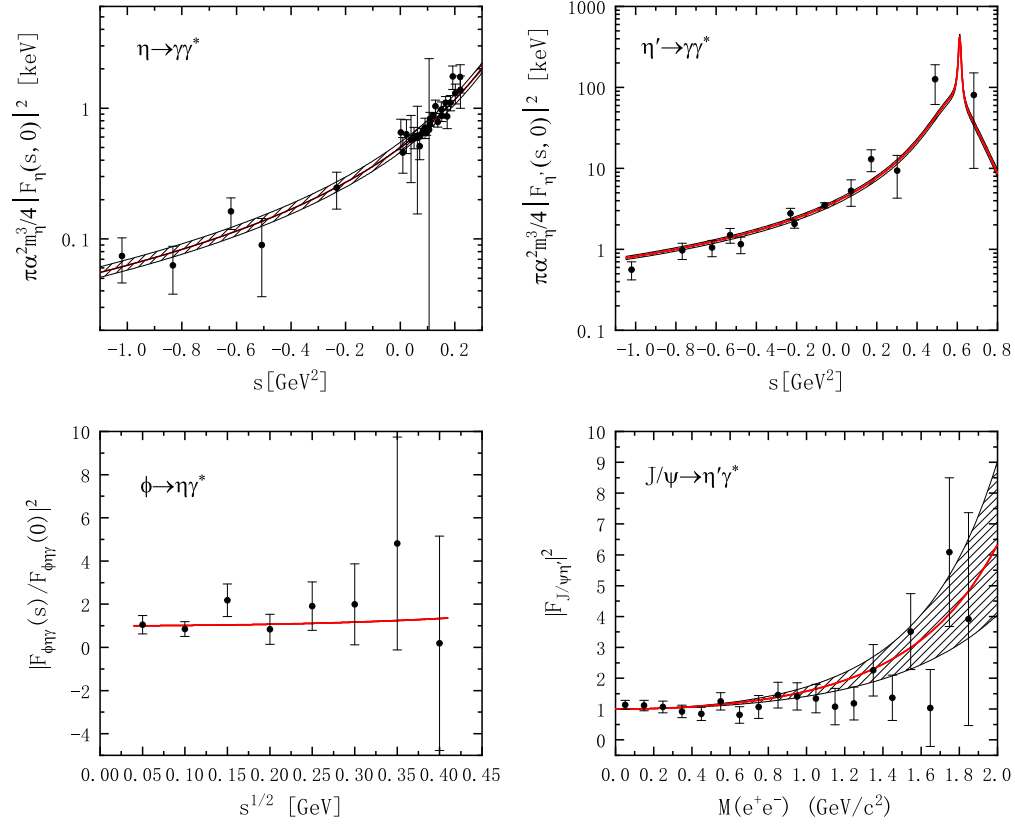


FIG. 4. The form factors for the $\eta \rightarrow \gamma\gamma^*$, $\eta' \rightarrow \gamma\gamma^*$, $\phi \rightarrow \eta\gamma^*$, and $J/\psi \rightarrow \eta'\gamma^*$. The red solid lines are obtained by taking the central values of the parameters in Table I, and the shaded areas correspond to the error bands at 1- σ level. The experimental data on the form factors for the $\eta \rightarrow \gamma\gamma^*$, $\eta' \rightarrow \gamma\gamma^*$, $\phi \rightarrow \eta\gamma^*$ and $J/\psi \rightarrow \eta'\gamma^*$ are taken from Refs. [45–50], Refs. [45–47,50,51], Ref. [48], and Ref. [44], respectively.

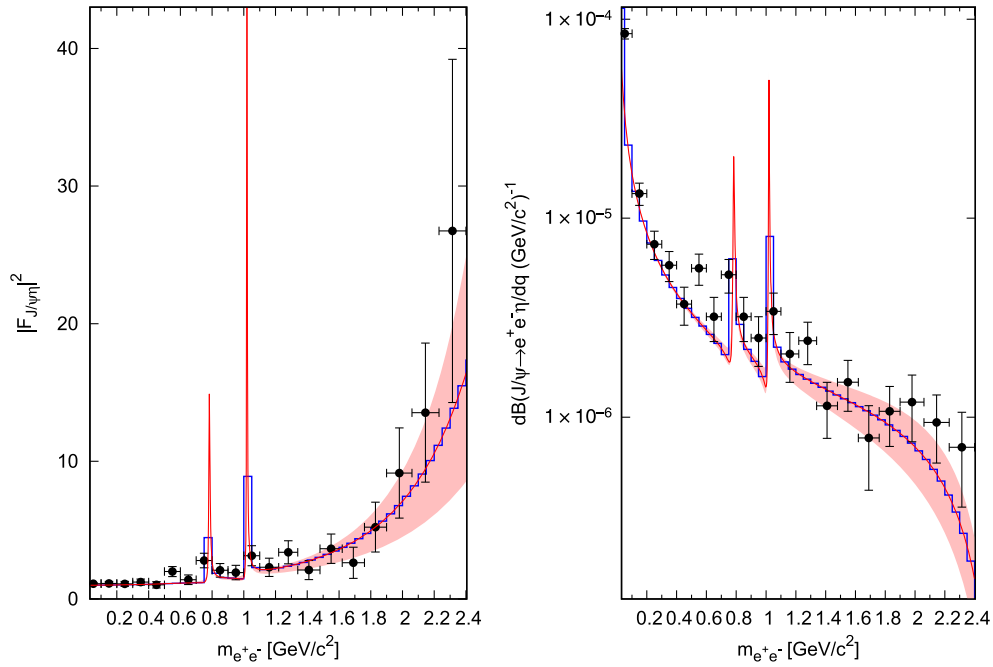


FIG. 5. The form factors and differential branching fractions for the $J/\psi \rightarrow \eta e^+ e^-$. The experimental data are from the Ref. [21]. The red solid lines represent the curves with the central values of the parameters in Table I, and the shaded areas stand for the error bands. The histograms are obtained by taking energy bin width at 50 MeV.

With the fitted parameters in Table I, it is then interesting to decipher the roles of different mechanisms and resonances played in a given process.

The $J/\psi \rightarrow Pl^+l^-$ processes can provide an environment to study the intermediate hadron resonances [20,52]. Recently, the $J/\psi \rightarrow \eta\gamma^*(\rightarrow e^+e^-)$ form factors are reported by the BESIII collaboration in Ref. [21], in which the experimental analysis includes only the ρ resonance in the e^+e^- spectra, apart from the QED contributions. However, it is pointed out that the ρ contribution should come from an isospin violated intermediate process $J/\psi \rightarrow \eta\rho \rightarrow \eta e^+e^-$. In contrast, the contributions from the ω and ϕ are expected to be more important, since they enter via the isospin conserved intermediate processes $J/\psi \rightarrow \eta\omega$ and $J/\psi \rightarrow \eta\phi$, whose branching ratios are around eight and four times larger than that of the $J/\psi \rightarrow \rho\eta$ in order. As a result, we expect that the effect of the ρ resonance is much suppressed, compared to the contributions from ω and ϕ . Due to the narrow widths of the latter two resonances, they manifest themselves as prominent peaks in the e^+e^- spectra, as shown in Fig. 5. However, these narrow peaks can be easily washed out when the energy resolution is low. E.g., we also explicitly give the energy distributions of the e^+e^- in Fig. 5 when taking the energy bin width at 50 MeV. In the latter case the

signals of the narrow ω and ϕ become fairly visible. As pointed out in Refs. [20,40,53], we also confirm the importance of the $\eta^{(\prime)} - \eta_c$ mixing mechanism in the $J/\psi \rightarrow \eta^{(\prime)}\gamma^{(*)}$ decay processes. A future experimental measurement with higher energy resolution will be definitely helpful to discriminate the roles of different hadrons in the $J/\psi \rightarrow \eta e^+e^-$ process. In Table V, we give our predictions to the branching ratios of various $J/\psi \rightarrow Pl^+l^-$ processes and also make comparisons with the results in Refs. [20,54,55].

Our study reveals an interesting feature that can shed light on the $\rho\pi$ puzzle in the $J/\psi(\psi') \rightarrow VP$ decays. For this purpose, let us focus on the interplay between the electromagnetic and strong interactions in the $J/\psi(\psi') \rightarrow VP$ processes. We separately show the contributions from the strong and electromagnetic interactions to the isospin conserved and violated decays for J/ψ and ψ' in Tables VI and VII, respectively. The contributions from the strong interactions are given by the $h_{i=1,2,3}$ terms in Eq. (14), while the electromagnetic contributions are obtained by taking $h_{i=1,2,3} = 0$. For the $J/\psi \rightarrow VP$ decays, the contributions from strong interactions turn out to play major roles in most of the isospin conserved channels, with the exception of the $J/\psi \rightarrow \phi\eta'$ process, where the strengths of the two types of interactions are comparable. While the isospin violated

TABLE V. Branching ratios ($\times 10^{-5}$) for $J/\psi \rightarrow Pl^+l^-$.

	Experiment	This Work	Ref. [20]	Ref. [54]	Ref. [55]
$\psi \rightarrow \pi^0 e^+ e^-$	0.076 ± 0.014	0.1294 ± 0.0044	0.1191 ± 0.0138	$0.0389^{+0.0037}_{-0.0033}$...
$\psi \rightarrow \eta e^+ e^-$	1.42 ± 0.08	1.35 ± 0.02	1.16 ± 0.08	1.21 ± 0.04	1.38
$\psi \rightarrow \eta' e^+ e^-$	6.59 ± 0.18	6.08 ± 0.05	5.76 ± 0.16	5.66 ± 0.16	6.06
$\psi \rightarrow \pi^0 \mu^+ \mu^-$...	0.0304 ± 0.0010	0.0280 ± 0.0032	$0.0101^{+0.0010}_{-0.0009}$...
$\psi \rightarrow \eta \mu^+ \mu^-$...	0.40 ± 0.01	0.32 ± 0.02	0.30 ± 0.01	0.46
$\psi \rightarrow \eta' \mu^+ \mu^-$...	1.64 ± 0.02	1.46 ± 0.04	1.31 ± 0.04	1.72

TABLE VI. The effective couplings of $G_{\psi \rightarrow VP}$ in units of 10^{-6} MeV^{-1} .

Isospin conserved cases	Experiment	Strong interaction	EM interaction
$ G_{J/\psi \rightarrow \rho^0 \pi^0} $	2.537 ± 0.154	2.899 ± 0.075	0.385 ± 0.006
$ G_{J/\psi \rightarrow \rho \pi} $	4.408 ± 0.191	5.022 ± 0.129	0.709 ± 0.009
$ G_{J/\psi \rightarrow \omega \eta} $	1.497 ± 0.084	1.586 ± 0.037	0.132 ± 0.009
$ G_{J/\psi \rightarrow \omega \eta'} $	0.562 ± 0.026	0.647 ± 0.028	0.119 ± 0.008
$ G_{J/\psi \rightarrow \phi \eta} $	1.060 ± 0.056	1.270 ± 0.045	0.198 ± 0.031
$ G_{J/\psi \rightarrow \phi \eta'} $	0.974 ± 0.052	1.074 ± 0.049	2.031 ± 0.044
$ G_{J/\psi \rightarrow K^{*+} K^-} $	2.011 ± 0.161	2.313 ± 0.048	0.216 ± 0.036
$ G_{J/\psi \rightarrow K^{*0} \bar{K}^0} $	1.686 ± 0.078	2.308 ± 0.048	0.715 ± 0.009
Isospin violated cases	Experiment	EM interaction	Strong interaction
$ G_{J/\psi \rightarrow \rho^0 \eta} $	0.498 ± 0.029	0.487 ± 0.028	...
$ G_{J/\psi \rightarrow \rho^0 \eta'} $	0.367 ± 0.018	0.365 ± 0.017	...
$ G_{J/\psi \rightarrow \omega \pi^0} $	0.721 ± 0.039	0.720 ± 0.035	...

TABLE VII. The effective couplings of $G_{\psi' \rightarrow VP}$ in units of 10^{-6} MeV^{-1} .

Isospin conserved cases	Experiment	Strong interaction	EM interaction
$ G_{\psi' \rightarrow \rho\pi} $	0.255 ± 0.044	0.029 ± 0.036	0.255 ± 0.016
$ G_{\psi' \rightarrow \omega\eta} $...	0.103 ± 0.038	0.036 ± 0.003
$ G_{\psi' \rightarrow \omega\eta'} $	0.288 ± 0.096	0.212 ± 0.079	0.079 ± 0.013
$ G_{\psi' \rightarrow \phi\eta} $	0.275 ± 0.013	0.285 ± 0.030	0.565 ± 0.029
$ G_{\psi' \rightarrow \phi\eta'} $	0.213 ± 0.013	0.197 ± 0.068	0.412 ± 0.067
$ G_{\psi' \rightarrow K^{*+}K^-} $	0.181 ± 0.012	0.263 ± 0.021	0.093 ± 0.021
$ G_{\psi' \rightarrow K^{*0}\bar{K}^0} $	0.352 ± 0.031	0.267 ± 0.021	0.568 ± 0.007
Isospin violated cases	Experiment	EM interaction	Strong interaction
$ G_{\psi' \rightarrow \rho^0\eta} $	0.219 ± 0.028	0.216 ± 0.026	...
$ G_{\psi' \rightarrow \rho^0\eta'} $	0.222 ± 0.083	0.271 ± 0.040	...
$ G_{\psi' \rightarrow \omega\pi^0} $	0.207 ± 0.028	0.208 ± 0.019	...

channels can only receive contributions from the electromagnetic interactions, since the isospin breaking effects from the strong interaction parts are not included in this work. According to the results shown in Table VII, for the $\psi' \rightarrow VP$ processes, the strong interactions are found to play comparable roles in many of the isospin conserved channels as those from the electromagnetic parts. Especially, the electromagnetic interaction turns out to play the dominant role in the $\psi' \rightarrow \rho\pi$ process and the effects from the strong interactions are found to be very small. In contrast, the strong interactions dominate the decay of $J/\psi \rightarrow \rho\pi$ process and the electromagnetic effects appear to be small. This provides a sensible explanation to the $\rho\pi$ puzzle.

For the charged $K^{*+}K^- + \text{c.c.}$ and neutral $K^{*0}\bar{K}^0 + \text{c.c.}$ decay processes of J/ψ or ψ' , the $SU(3)$ breaking effects can originate from the strong interactions via the h_2 term in Eq. (14), which turns out to be the same for both charged and neutral processes, and the electromagnetic interactions via the c_j terms in Eq. (12), where the c_4 operator is found to solely contribute to the charged process [19]. The contributions from the electromagnetic parts to the $J/\psi \rightarrow K^*\bar{K} + \text{c.c.}$ processes are obviously smaller than those from the strong interactions, which explains the similar branching ratios between $J/\psi \rightarrow K^{*+}K^- + \text{c.c.}$ and $J/\psi \rightarrow K^{*0}\bar{K}^0 + \text{c.c.}$ In contrast, our study reveals that the magnitudes of the strong interactions in the $\psi' \rightarrow K^*\bar{K} + \text{c.c.}$ can be comparable with those of the electromagnetic parts. While, the $SU(3)$ breaking effects in the electromagnetic parts are quite different for the charged and neutral decay processes due to the c_4 operator [19]. This gives a new insight and also a reasonable explanation to the very different branching ratios of the $\psi' \rightarrow K^{*+}K^- + \text{c.c.}$ and $\psi' \rightarrow K^{*0}\bar{K}^0 + \text{c.c.}$

IV. SUMMARY AND CONCLUSIONS

We use the effective Lagrangian approach to simultaneously investigate the processes of $J/\psi(\psi') \rightarrow VP$,

$J/\psi \rightarrow P\gamma, J/\psi \rightarrow Pl^+l^-$, the radiative decays of light-flavor hadrons and their relevant form factors. High energy constraints on the resonance couplings are used to reduce the number of free parameters. The remaining resonance couplings are then determined through the joint fit to a large amount of experimental data, including the updated PDG averages of the various partial decay widths and the most recent $J/\psi \rightarrow \eta\gamma^*$ form factors from BESIII.

Thanks to the use of effective Lagrangian, the different types of contributions from the OZI allowed/suppressed strong interactions, $SU(3)$ breaking terms and electromagnetic effects can be easily identified in our study. We pay special attention to the relative magnitudes from the strong and electromagnetic interactions in the $J/\psi \rightarrow VP$ and $\psi' \rightarrow VP$ processes, so as to provide an insight into the $\rho\pi$ puzzle. An anatomy of the $J/\psi \rightarrow \rho\pi$ and $\psi' \rightarrow \rho\pi$ amplitudes reveals that the strong interaction dominates the former process and the electromagnetic interaction prevails the latter one. For the obviously distinct ratios between the charged $B(\psi' \rightarrow K^{*+}K^- + \text{c.c.})/B(J/\psi \rightarrow K^{*+}K^- + \text{c.c.})$ and the neutral $B(\psi' \rightarrow K^{*0}\bar{K}^0 + \text{c.c.})/B(J/\psi \rightarrow K^{*0}\bar{K}^0 + \text{c.c.})$ processes, our study uncovers that the $J/\psi \rightarrow K^*\bar{K} + \text{c.c.}$ processes are mainly ruled by the strong interactions, where the $SU(3)$ breaking effects enter similarly in both the charged and neutral amplitudes, while the $\psi' \rightarrow K^*\bar{K} + \text{c.c.}$ decays are found to be importantly affected by the electromagnetic interactions, where the $SU(3)$ symmetry breaking terms appear differently in the charged and neutral processes.

ACKNOWLEDGMENTS

We thank Lu Niu for an early-stage contribution to this work. This work is partially funded by the Natural Science Foundation of China under Grants No. 11975090, No. 12150013, No. 11975028, and No. 11974043, and the Science Foundation of Hebei Normal University.

APPENDIX: THE EXPRESSIONS OF THE EFFECTIVE COUPLINGS FOR $\psi' \rightarrow VP$

The expressions of the effective couplings in the $\psi' \rightarrow VP$ processes defined in Eq. (20) take the form:

$$G_{\psi' \rightarrow \rho^0 \pi^0} = \frac{2\sqrt{2}}{F_\pi M_\rho} h'_1 M_{\psi'} + \frac{8\sqrt{2}}{F_\pi M_\rho} h'_2 m_\pi^2 \frac{1}{M_{\psi'}} + \frac{32\pi\alpha}{F_\pi M_\rho} F_V g'_1 + \frac{128\pi\alpha}{F_\pi M_\rho} F_V g'_2 \frac{m_\pi^2}{M_{\psi'}^2} + \frac{8\sqrt{2}\pi\alpha}{3} \frac{f_{\psi'}}{M_{\psi'}} F_{\rho\pi\gamma^*}(M_{\psi'}^2), \quad (\text{A1})$$

$$G_{\psi' \rightarrow \rho^+ \pi^-} = \frac{2\sqrt{2}}{F_\pi M_\rho} h'_1 M_{\psi'} + \frac{8\sqrt{2}}{F_\pi M_\rho} h'_2 m_\pi^2 \frac{1}{M_{\psi'}} + \frac{8\sqrt{2}\pi\alpha}{3} \frac{f_{\psi'}}{M_{\psi'}} F_{\rho\pi\gamma^*}(M_{\psi'}^2), \quad (\text{A2})$$

$$G_{\psi' \rightarrow \rho^0 \eta} = \frac{32\sqrt{2}\pi\alpha}{3FM_\rho} F_V g'_1 (a_1 - a_3) + \frac{128\sqrt{2}\pi\alpha}{3FM_\rho M_{\psi'}^2} F_V g'_2 [a_1 m_\pi^2 - a_3 (2m_K^2 - m_\pi^2)] - 8\pi\alpha \frac{F_V}{M_\rho} \lambda_{\eta c} g_{\psi' \eta c \gamma^*}(M_\rho^2) e^{i\delta'_\eta} + \frac{8\sqrt{2}\pi\alpha}{3} \frac{f_{\psi'}}{M_{\psi'}} F_{\rho\eta\gamma^*}(M_{\psi'}^2), \quad (\text{A3})$$

$$G_{\psi' \rightarrow \rho^0 \eta'} = \frac{32\sqrt{2}\pi\alpha}{3FM_\rho} F_V g'_1 (a_2 - a_4) + \frac{128\sqrt{2}\pi\alpha}{3FM_\rho M_{\psi'}^2} F_V g'_2 [a_2 m_\pi^2 - a_4 (2m_K^2 - m_\pi^2)] - 8\pi\alpha \frac{F_V}{M_\rho} \lambda_{\eta' c} g_{\psi' \eta' c \gamma^*}(M_\rho^2) e^{i\delta'_{\eta'}} + \frac{8\sqrt{2}\pi\alpha}{3} \frac{f_{\psi'}}{M_{\psi'}} F_{\rho\eta'\gamma^*}(M_{\psi'}^2), \quad (\text{A4})$$

$$G_{\psi' \rightarrow \omega \pi^0} = \frac{32\pi\alpha}{3F_\pi M_\omega} F_V g'_1 + \frac{128\pi\alpha}{3F_\pi M_\omega} F_V g'_2 \frac{m_\pi^2}{M_{\psi'}^2} + \frac{8\sqrt{2}\pi\alpha}{3} \frac{f_{\psi'}}{M_{\psi'}} F_{\omega\pi\gamma^*}(M_{\psi'}^2), \quad (\text{A5})$$

$$G_{\psi' \rightarrow \omega \eta} = \frac{4}{FM_\omega} a_1 h'_1 M_{\psi'} + \frac{16}{FM_\omega} a_1 h'_2 m_\pi^2 \frac{1}{M_{\psi'}} + \frac{4}{FM_\omega} (2a_1 + a_3) h'_3 M_{\psi'} + \frac{32\sqrt{2}\pi\alpha}{9FM_\omega} F_V g'_1 (a_1 - a_3) + \frac{128\sqrt{2}\pi\alpha}{9FM_\omega M_{\psi'}^2} F_V g'_2 [a_1 m_\pi^2 - a_3 (2m_K^2 - m_\pi^2)] - \frac{8}{3} \pi\alpha \frac{F_V}{M_\omega} \lambda_{\eta c} g_{\psi' \eta c \gamma^*}(M_\omega^2) e^{i\delta'_\eta} + \frac{8\sqrt{2}\pi\alpha}{3} \frac{f_{\psi'}}{M_{\psi'}} F_{\omega\eta\gamma^*}(M_{\psi'}^2), \quad (\text{A6})$$

$$G_{\psi' \rightarrow \omega \eta'} = \frac{4}{FM_\omega} a_2 h'_1 M_{\psi'} + \frac{16}{FM_\omega} a_2 h'_2 m_\pi^2 \frac{1}{M_{\psi'}} + \frac{4}{FM_\omega} (2a_2 + a_4) h'_3 M_{\psi'} + \frac{32\sqrt{2}\pi\alpha}{9FM_\omega} F_V g'_1 (a_2 - a_4) + \frac{128\sqrt{2}\pi\alpha}{9FM_\omega M_{\psi'}^2} F_V g'_2 [a_2 m_\pi^2 - a_4 (2m_K^2 - m_\pi^2)] - \frac{8}{3} \pi\alpha \frac{F_V}{M_\omega} \lambda_{\eta' c} g_{\psi' \eta' c \gamma^*}(M_\omega^2) e^{i\delta'_{\eta'}} + \frac{8\sqrt{2}\pi\alpha}{3} \frac{f_{\psi'}}{M_{\psi'}} F_{\omega\eta'\gamma^*}(M_{\psi'}^2), \quad (\text{A7})$$

$$G_{\psi' \rightarrow \phi \eta} = -\frac{2\sqrt{2}}{FM_\phi} a_3 h'_1 M_{\psi'} - \frac{8\sqrt{2}}{FM_\phi} a_3 h'_2 (2m_K^2 - m_\pi^2) \frac{1}{M_{\psi'}} - \frac{2\sqrt{2}}{FM_\phi} (2a_1 + a_3) h'_3 M_{\psi'} + \frac{64\pi\alpha}{9FM_\phi} F_V g'_1 (a_1 - a_3) + \frac{256\pi\alpha}{9FM_\phi M_{\psi'}^2} F_V g'_2 [a_1 m_\pi^2 - a_3 (2m_K^2 - m_\pi^2)] - \frac{8\sqrt{2}}{3M_\phi} \pi\alpha F_V \lambda_{\eta c} g_{\psi' \eta c \gamma^*}(M_\phi^2) e^{i\delta'_\eta} + \frac{8\sqrt{2}\pi\alpha}{3} \frac{f_{\psi'}}{M_{\psi'}} F_{\phi\eta\gamma^*}(M_{\psi'}^2), \quad (\text{A8})$$

$$G_{\psi' \rightarrow \phi \eta'} = -\frac{2\sqrt{2}}{FM_\phi} a_4 h'_1 M_{\psi'} - \frac{8\sqrt{2}}{FM_\phi} a_4 h'_2 (2m_K^2 - m_\pi^2) \frac{1}{M_{\psi'}} - \frac{2\sqrt{2}}{FM_\phi} (2a_2 + a_4) h'_3 M_{\psi'} + \frac{64\pi\alpha}{9FM_\phi} F_V g'_1 (a_2 - a_4) + \frac{256\pi\alpha}{9FM_\phi M_{\psi'}^2} F_V g'_2 [a_2 m_\pi^2 - a_4 (2m_K^2 - m_\pi^2)] - \frac{8\sqrt{2}}{3M_\phi} \pi\alpha F_V \lambda_{\eta' c} g_{\psi' \eta' c \gamma^*}(M_\phi^2) e^{i\delta'_{\eta'}} + \frac{8\sqrt{2}\pi\alpha}{3} \frac{f_{\psi'}}{M_{\psi'}} F_{\phi\eta'\gamma^*}(M_{\psi'}^2), \quad (\text{A9})$$

$$G_{\psi' \rightarrow K^{*+} K^-} = \frac{2\sqrt{2}}{F_K M_{K^*}} h'_1 M_{\psi'} + \frac{8\sqrt{2}}{F_K M_{K^*}} h'_2 m_K^2 \frac{1}{M_{\psi'}} + \frac{8\sqrt{2}\pi\alpha}{3} \frac{f_{\psi'}}{M_{\psi'}} F_{K^{*+} K^- \gamma^*}(M_{\psi'}^2), \quad (\text{A10})$$

$$G_{\psi' \rightarrow K^{*0} \bar{K}^0} = \frac{2\sqrt{2}}{F_K M_{K^*}} h'_1 M_{\psi'} + \frac{8\sqrt{2}}{F_K M_{K^*}} h'_2 m_K^2 \frac{1}{M_{\psi'}} + \frac{8\sqrt{2}\pi\alpha}{3} \frac{f_{\psi'}}{M_{\psi'}} F_{K^{*0} \bar{K}^0 \gamma^*}(M_{\psi'}^2), \quad (\text{A11})$$

with

$$\begin{aligned} a_1 &= \frac{F}{\cos(\theta_0 - \theta_8)} \left(\frac{\cos \theta_0}{\sqrt{6} F_8} - \frac{\sin \theta_8}{\sqrt{3} F_0} \right), \\ a_2 &= \frac{F}{\cos(\theta_0 - \theta_8)} \left(\frac{\sin \theta_0}{\sqrt{6} F_8} + \frac{\cos \theta_8}{\sqrt{3} F_0} \right), \\ a_3 &= \frac{F}{\cos(\theta_0 - \theta_8)} \left(\frac{-2 \cos \theta_0}{\sqrt{6} F_8} - \frac{\sin \theta_8}{\sqrt{3} F_0} \right), \\ a_4 &= \frac{F}{\cos(\theta_0 - \theta_8)} \left(\frac{-2 \sin \theta_0}{\sqrt{6} F_8} + \frac{\cos \theta_8}{\sqrt{3} F_0} \right). \end{aligned} \quad (\text{A12})$$

The expressions $F_{K^{*+} K^- \gamma^*}$ and $F_{K^{*0} \bar{K}^0 \gamma^*}$ that correspond to the electromagnetic contributions to the effective couplings of $G_{\psi' \rightarrow K^{*+} K^-}$ and $G_{\psi' \rightarrow K^{*0} \bar{K}^0}$ are given by

$$\begin{aligned} F_{K^{*+} K^- \gamma^*}(s) &= \frac{-2\sqrt{2}}{3F_K M_V M_{K^*}} [(c_1 + c_2 + 8c_3 - c_5)m_K^2 + (c_2 + c_5 - c_1 - 2c_6)M_{K^*}^2 + (c_1 - c_2 + c_5)s \\ &\quad + 24c_4(m_K^2 - m_\pi^2)] + \frac{2F_V}{3F_K M_{K^*}} [(d_1 + 8d_2 - d_3)m_K^2 + d_3(M_{K^*}^2 + s)][D_\omega(s) + 3D_\rho(s) - 2D_\phi(s)], \end{aligned} \quad (\text{A13})$$

and

$$\begin{aligned} F_{K^{*0} \bar{K}^0 \gamma^*}(s) &= \frac{4\sqrt{2}}{3F_K M_V M_{K^*}} [(c_1 + c_2 + 8c_3 - c_5)m_K^2 + (c_2 + c_5 - c_1 - 2c_6)M_{K^*}^2 + (c_1 - c_2 + c_5)s] \\ &\quad + \frac{2F_V}{3F_K M_{K^*}} [(d_1 + 8d_2 - d_3)m_K^2 + d_3(M_{K^*}^2 + s)][D_\omega(s) - 3D_\rho(s) - 2D_\phi(s)]. \end{aligned} \quad (\text{A14})$$

It is pointed out that $SU(3)$ breaking effect caused by the c_4 term only enters in the charged $F_{K^{*+} K^- \gamma^*}$ amplitude and is absent in the neutral $F_{K^{*0} \bar{K}^0 \gamma^*}$ process. For the expressions of other amplitudes $F_{VP\gamma^*}$, they are given in Appendix of Ref. [20] and we do not repeat them here.

-
- | | |
|---|--|
| [1] T. Appelquist, A. De Rujula, H. D. Politzer, and S. L. Glashow, <i>Phys. Rev. Lett.</i> 34 , 365 (1975). | [8] S. J. Brodsky and M. Karliner, <i>Phys. Rev. Lett.</i> 78 , 4682 (1997). |
| [2] T. Appelquist and H. D. Politzer, <i>Phys. Rev. Lett.</i> 34 , 43 (1975). | [9] S. S. Pinsky, <i>Phys. Lett. B</i> 236 , 479 (1990). |
| [3] A. De Rujula and S. L. Glashow, <i>Phys. Rev. Lett.</i> 34 , 46 (1975). | [10] T. Feldmann and P. Kroll, <i>Phys. Rev. D</i> 62 , 074006 (2000). |
| [4] R. L. Workman <i>et al.</i> (Particle Data Group), <i>Prog. Theor. Exp. Phys.</i> 2022 , 083C01 (2022). | [11] X. Q. Li, D. V. Bugg, and B. S. Zou, <i>Phys. Rev. D</i> 55 , 1421 (1997). |
| [5] M. E. B. Franklin <i>et al.</i> , <i>Phys. Rev. Lett.</i> 51 , 963 (1983). | [12] Q. Zhao, <i>Phys. Lett. B</i> 697 , 52 (2011). |
| [6] M. Suzuki, <i>Phys. Rev. D</i> 63 , 054021 (2001). | [13] Q. Wang, G. Li, and Q. Zhao, <i>Phys. Rev. D</i> 85 , 074015 (2012). |
| [7] Y. Q. Chen and E. Braaten, <i>Phys. Rev. Lett.</i> 80 , 5060 (1998). | [14] J. M. Gerard and A. Martini, <i>Phys. Lett. B</i> 730 , 264 (2014). |
| | [15] G. 't Hooft, <i>Nucl. Phys.</i> B72 , 461 (1974); 75 , 461 (1974); E. Witten, <i>Nucl. Phys.</i> B160 , 57 (1979). |

- [16] J. Gasser and H. Leutwyler, *Ann. Phys. (N.Y.)* **158**, 142 (1984).
- [17] J. Gasser and H. Leutwyler, *Nucl. Phys.* **B250**, 465 (1985).
- [18] Y. H. Chen, Z. H. Guo, and H. Q. Zheng, *Phys. Rev. D* **85**, 054018 (2012).
- [19] Y. H. Chen, Z. H. Guo, and H. Q. Zheng, *Phys. Rev. D* **90**, 034013 (2014).
- [20] Y. H. Chen, Z. H. Guo, and B. S. Zou, *Phys. Rev. D* **91**, 014010 (2015).
- [21] M. Ablikim *et al.* (BESIII Collaboration), *Phys. Rev. D* **99**, 012006 (2019); **104**, 099901(E) (2021).
- [22] G. Ecker, J. Gasser, A. Pich, and E. de Rafael, *Nucl. Phys.* **B321**, 311 (1989).
- [23] V. Cirigliano, G. Ecker, M. Eidemuller, R. Kaiser, A. Pich, and J. Portoles, *Nucl. Phys.* **B753**, 139 (2006).
- [24] E. Witten, *Nucl. Phys.* **B156**, 269 (1979); S. R. Coleman and E. Witten, *Phys. Rev. Lett.* **45**, 100 (1980); G. Veneziano, *Nucl. Phys.* **B159**, 213 (1979).
- [25] H. Leutwyler, *Nucl. Phys. B, Proc. Suppl.* **64**, 223 (1998).
- [26] R. Kaiser and H. Leutwyler, [arXiv:hep-ph/9806336](https://arxiv.org/abs/hep-ph/9806336).
- [27] G. Ecker, J. Gasser, H. Leutwyler, A. Pich, and E. de Rafael, *Phys. Lett. B* **223**, 425 (1989).
- [28] P. D. Ruiz-Femenia, A. Pich, and J. Portoles, *J. High Energy Phys.* **07** (2003) 003.
- [29] K. Kampf and J. Novotny, *Phys. Rev. D* **84**, 014036 (2011).
- [30] J. A. Miranda and P. Roig, *Phys. Rev. D* **102**, 114017 (2020).
- [31] K. T. Chao, *Nucl. Phys.* **B335**, 101 (1990).
- [32] J. J. Dudek, R. G. Edwards, and D. G. Richards, *Phys. Rev. D* **73**, 074507 (2006).
- [33] J. J. Dudek, R. Edwards, and C. E. Thomas, *Phys. Rev. D* **79**, 094504 (2009).
- [34] Y. Chen, D. C. Du, B. Z. Guo, N. Li, C. Liu, H. Liu, Y. B. Liu, J. P. Ma, X. F. Meng, Z. Y. Niu *et al.*, *Phys. Rev. D* **84**, 034503 (2011).
- [35] Z. H. Guo and P. Roig, *Phys. Rev. D* **82**, 113016 (2010).
- [36] P. Roig and J. J. Sanz Cillero, *Phys. Lett. B* **733**, 158 (2014).
- [37] C. Chen, C. G. Duan, and Z. H. Guo, *J. High Energy Phys.* **08** (2022) 144.
- [38] Z. H. Guo and J. A. Oller, *Phys. Rev. D* **84**, 034005 (2011).
- [39] For a review see, T. Feldmann, *Int. J. Mod. Phys. A* **15**, 159 (2000).
- [40] Q. Zhao, *Phys. Lett. B* **697**, 52 (2011).
- [41] T. Feldmann, P. Kroll, and B. Stech, *Phys. Rev. D* **58**, 114006 (1998).
- [42] A. Bramon, R. Escribano, and M. D. Scadron, *Phys. Lett. B* **403**, 339 (1997).
- [43] R. Escribano, *Eur. Phys. J. C* **65**, 467 (2010).
- [44] M. Ablikim *et al.* (BESIII Collaboration), *Phys. Rev. D* **89**, 092008 (2014).
- [45] R. I. Dzhelyadin *et al.*, *Phys. Lett.* **94B**, 548 (1980).
- [46] R. I. Dzhelyadin *et al.*, *Phys. Lett.* **88B**, 379 (1979).
- [47] H. J. Behrend *et al.* (CELLO Collaboration), *Z. Phys. C* **49**, 401 (1991).
- [48] M. N. Achasov *et al.*, *Phys. Lett. B* **504**, 275 (2001).
- [49] R. Arnaldi *et al.* (NA60 Collaboration), *Phys. Lett. B* **677**, 260 (2009).
- [50] H. Aihara *et al.* (TPC/Two Gamma Collaboration), *Phys. Rev. Lett.* **64**, 172 (1990).
- [51] M. Acciarri *et al.* (L3 Collaboration), *Phys. Lett. B* **418**, 399 (1998).
- [52] B. Kubis and F. Niecknig, *Phys. Rev. D* **91**, 036004 (2015).
- [53] Kuang-Ta Chao, *Nucl. Phys.* **B335**, 101 (1990).
- [54] J. Fu, H. B. Li, X. Qin, and M. Z. Yang, *Mod. Phys. Lett. A* **27**, 1250223 (2012).
- [55] J. K. He and C. J. Fan, *Phys. Rev. D* **105**, 094034 (2022).